

Green Chemistry Synthesis of Nano-Hydroxyapatite using Natural Stabilisers

Sreedevi Nimishakavi^{1,*}, V. Madhusudhan Rao¹, A. K. Singh²

¹Vignans Foundation for Science, Technology & Research, Guntur -Tenali Rd, Vadlamudi, Andhra Pradesh 522213, India

²Defence Metallurgical Research Laboratory, Kanchan Bagh, Hyderabad, Telangana 500066, India

*Corresponding author: E-mail: nsdm2013@gmail.com, Tel.: (+91) 9441822952

DOI: 10.5185/amlett.2021.031610

Present work describes the synthesis and characterization of Nano-Hydroxyapatite (nano-HAP) powders through green chemistry route, using Natural Stabilizers (NS) as precursors. The synthesized powders possess crystallite and particles of sizes in nano range. The nature of the powder is poly dispersive. The morphology of synthesized powders is near spherical and the pH value is greater than the ten. The powder possesses similar dielectric constant value of 100 Hz at room temperature, as reported in literature. The corresponding wave numbers of the nano-HAP powder match with the reported functional groups.

Introduction

There is a great increase of awareness in the field of dentistry during the last four decades. As such, a large number of programs have been initiated to develop biocompatible materials that can mimic naturally existing dental materials [1]. Hydroxyapatite (HAP) is an important biomaterial with chemical formula $\text{Ca}_{10}(\text{PO}_4)_6(\text{OH})_2$ that has greater similarity to bones and teeth [2]. Synthetic HAP can imitate natural dental Hydroxyapatite or enamel apatite [3-5]. Nano-HAP has been considered as a repairing material by NASA and the rights were purchased by the Japanese Company, Sangi Co. Ltd. in 1970 [6]. It has launched a tooth paste for the first time that could repair the tooth enamel which contains Nano-HAP, (Apadent) in 1978. The toothpastes containing n-HAP have revealed higher remineralisation effects with in vitro conditions chosen in comparison to that of the amine fluoride toothpaste with bovine dentin. As a result, the comparable trends are obtained for enamel [7].

The nano-HAPs have been extensively used in periodontology and maxillofacial surgery owing to its unique properties such as ability to bind to bone and to facilitate bone growth (a direct action on Osteoblasts) [8]. It is totally biomimetic which means human body recognises it as familiar structure that belongs there due to its wonderful biocompatibility [7]. It has been reported that it encourages the bone to grow and restores the defect due to its associated bioactivities. Therefore, the Calcium Phosphate nanoparticles can be considered as safe for humans since the risk associated with this is significantly low [9].

It has been proved that the nano-HAP can be utilized for enamel repair [10]. In 2006, the first toothpaste containing synthetic nano-HAP bio mimetic as an alternative to fluoride for the remineralisation and repair of tooth enamel, appeared in Europe [6-7]. It can protect and create a new layer of enamel around the tooth, rather

than the hardening layer like Calciumhalophosphate [$\text{Ca}_3(\text{PO}_4)_3\text{F}$] [6,7,10,11].

The nano-HAP can improve the biocompatible properties that can bind with the tooth and induces no phenomena of toxicity or inflammatory, local or systemic. Some researches show that it does not undergo resorption unlike tri-calcium phosphate. Numerous studies have highlighted the role of nano-HAP in facilitating the osteo-integration with or without other polymeric space [12]. Nano-HAP is, in fact, a better source of free Ca, and this is a key element as regards the remineralisation, protection against caries and dental erosion [13]. Research developments have led to add 0.25% of nano-HAP in beverages such as mineral supplements for sports activities, in order to prevent tooth erosion caused by consuming these beverages during the stop gaps in sports [14]. A continuing interest in nano-HAP has led the researchers to look forward for new combinations that can meet the needs of dental materials.

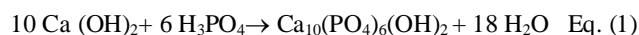
Present work is thus concerned with synthesis of nano-HAP through green chemistry route and subsequent characterization. The synthesis of nano-HAP in present work has been carried out using rice water solution as natural stabilizer (NS) precursors. A modification to prepare nano-HAP using NS as precursor is developed using sol-gel method with different concentrations. The main objective for the preparation of nano-HAP using NS is to develop eco-friendly biomaterial that can give rise to smaller particle size due to the capping process and also reducing agglomeration. The selection of a particular precursor depends on its dispersive ability.

Experimental section

Material preparation

Aqueous based synthesis is one of the popular methods of preparation of nano-HAP. This was prepared through wet chemical precipitation method. The shape, size and specific surface area of the nano-HAP obtained by this

method is very sensitive to the reactants addition rate and the reaction temperature. Ortho-phosphoric acid is then added to aqueous calcium hydroxide. It is an acid- base neutralisation which is an exothermic reaction. The reaction is proposed by Yagai and Aoki as directed by Bouyer *et. al.*, [15]. The initial temperature of the reaction is noted as 83 °C and it returns to room temperature in 18 minutes.



Ammonium Hydroxide is used as a leaving agent or acidity regulator in food and drug administration and is generally recognised as a safe reagent. Its pH controlling abilities make it an effective antimicrobial agent. Aqueous ammonia is an excellent acid neutraliser.

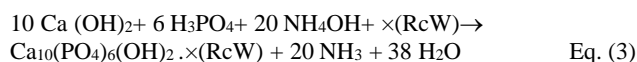


In the present study, a new method is developed to prepare Nano-Hydroxyapatite using natural stabilisers (NS) of different concentrations. There is no specific criterion for the amount of reducing agent required, type of NS and the optimum concentration. The most commonly available material is the by-product of staple food of Indians i.e. rice water (RcW). The RcW is a specific NS which is a non-inflammatory substance and works as a dispersant to control the agglomeration process of end product of equation (2) at different concentrations. It acts as a capping agent in the present reaction and reduces the crystallite size with increase in concentration of the NS. As a result, the different concentrations of RcW solutions namely, 5, 10 and 15ml were utilized in present study for resultant product at 30, 40 and 50 °C. It is to be noted that the products obtained via equations (1) and (2) result in nano-sized HAP [15].

Modification

A low temperature water-based sol – gel process for nano-HAP synthesis has been developed previously, using triethyl Phosphate and calcium nitrate as phosphorus and calcium precursors, respectively [15,16].

There is no specific rule or a definite measure with regard to the optimum concentration or proportion of the NS to be used in synthesis of nano-HAP. The nature of material used as NS is responsible for preventing uncountable growth, agglomeration and size of product [powders nano-particles (NPs)]. The concentration and proportion of the NS, in turn control the size of the resulting particles. The RcW is a healthy solution which contains chock full of vitamins, minerals and amino acids. It is also very much cost effective. In addition, it is a powerful antioxidant which contains anti-inflammatory properties. Thick cloudy white water from cooked rice is used as a NS. Modified synthesis is based on the homogeneous precipitation technique. Addition of the RcW decreases initial temperature of the reaction and changes rate of reaction. The reaction time increases as the concentration of the NS increases. The modified equation (2) with addition of RcW as NS is given in equation (3).



where \times is the number of moles of RcW solution used in equation (3). These are 5, 10 and 15 ml in present study.

Material characterization

The powders obtained using equation (3) were subjected to X-ray diffraction (XRD) studies in INEL (France) equinox 3000 equipment attached with a copper source ($K\alpha$ radiation) and position-sensitive detector (PSD). The XRD equipment was operated at 40 kV and 30 mA. The XRD patterns were used to measure the crystallite sizes of the powders.

The shape and sizes of the particles were examined in scanning electron microscope (SEM). SEM studied were carried out in ZEISS equipment, EVO 18 special edition. Small angle X-ray scattering (SAXS) was used to measure the size, shape and distribution of the particles of derived powder. The equipment model and make are Xeuss 1.0, and Xenocs, France. It is operated with dual energy Mo and Cr micro source, with Camera length 2400 mm and q range: 0.024 to 14 nm^{-1} , where q is scattering wave vector. Dielectric constant properties were studied using high precision impedance analyzer (Model WK (WAYNE KERR), 6500B) in which the high temperature furnace is connected to a desktop interface. Rate of heating was 2 degrees /minute; the temperature was fixed in 4 slots that were room temperature (29 °C), 50, 75 and 100 °C and the frequency ranges were set between 50-5 MHz.

Fourier transform infrared spectroscopy (FTIR) was studied in order to obtain the spectrum in an FTIR instrument (MODEL: IRPrestige21, cat. No. 206 – 73600-36, serial no. A21005002961LP, Shimadzu Corporation, Kyoto Japan) that can be operated at 220V/230/240V~50/60Hz.

Results and discussion

Effect of NS as pH controller

The quality of a biomaterial depends on its pH value. The Size of Nano Particle (NP) changes due to the solubility of NS, rate of reaction, initial temperature and its pH. It is due to the strength of bonding between the surface of NPs and one end of the capping agent (CA). The values of pH were measured with pH meter with a measuring range 0.0 – 14.0. As nano-HAP particles were prepared using RcW as NS with 5, 10 and 15 ml concentrations, the steric repulsion provided by NS controls the agglomeration and their pH. The observed pH values, time of reaction and initial temperature on function of different volumes NS used nano-HAP are given in **Table 1**. It is clear from the table that that the addition of NS plays an important role in pH and morphology. It is known that pH above 10.0 possess the Ca/P ratio close to the stoichiometric HAP and the particles synthesised are of different sizes and dispersability [17].

This PH values are graphically displayed in **Fig. 1**. Both the pH value and time of reaction are lower in nano –

HAP of 5ml NS (RcW solution) than nano – HAP without NS. This reflects that 5 ml RcW NS initially decreases the pH and rate of reaction. Further increase in volume of RcW solution increases both the pH and rate of reaction. Interestingly, the increase in RcW solution decreases the initial temperature of the reaction. The 15ml RcW solution results in very high value of pH which can be employed as protective layer for dental applications.

Table 1. The observed pH values, time of reaction and initial temperature with different volumes of NS.

NS(RcW) (ml)	pH	Time (minute)	Initial Temp. (°C)
0	10.8	18	83
5	9.8	13	62
10	10.3	19	58
15	12.3	20	51

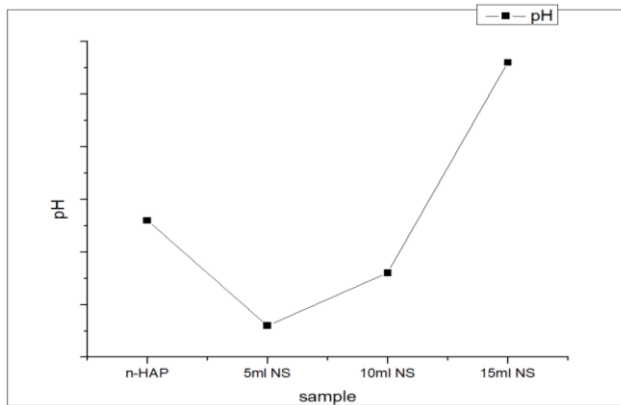


Fig. 1. Concentration of Natural Stabiliser used in the reaction of nano-HAP and relative pH changes.

XRD - Crystallite size

X-Ray Diffraction (XRD) has been used to determine the crystallite size of the nano- HAP material synthesised by the method described above. All the XRD patterns exhibit that the HAP could be synthesized at initial pH values higher than 10.0, despite of different purities and degrees of crystallinity. The data obtained is processed using Scherrer's formula to calculate the crystallite size [18]. The main diffraction peaks in this pattern match with the 2θ to relative planes of (211), (310), (222) etc.

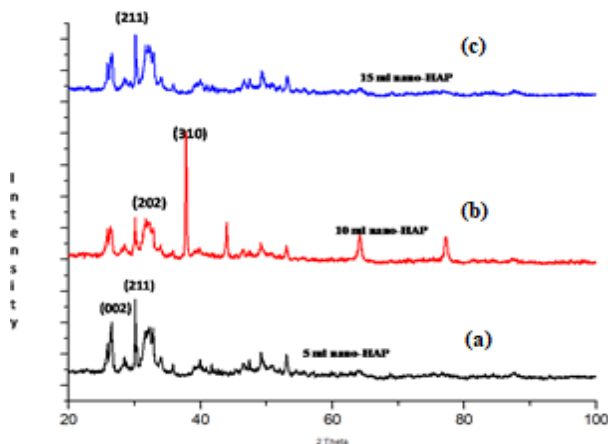


Fig. 2. XRD Patterns: (a) 5, (b) 10, and (c) 15RcW NS.

$$D_p = 0.94 \lambda / \beta \cos \Theta$$

Eq. (4)

Where

D_p = average crystallite size

λ = X- ray wavelength

β = FWHM of peak (line broadening in radians)

Θ = Bragg angle.

For this calculation 5 distinct peaks comparing to (211), (002), (111), (310) and (202) planes have been used. The calculated values of crystallite sizes are given in **Table 2.** The crystallite size of nano-HAP is calculated using the data of peak position and relative FWHM using equation (4).

Table 2. Crystallite size of nano-HAP using peak position and FWHM.

NS	Crystallite size (nm)					Ave. Crystallite size (nm)
	(211)	(002)	(111)	(310)	(202)	
0 ml	16.33	35.02	---	11.66	47.92	27.73
5 ml/30°C	27.02	15.91	---	42.64	23.32	27.22
10 ml/30°C	12.58	13.56	49.44	---	25.39	25.24
15 ml/30°C	6.72	21.07	18.00	4.98	---	12.69
5 ml/40°C	---	40.14	---	---	24.78	32.46
10 ml/40°C	18.08	39.22	---	23.48	20.56	25.34
15 ml/40°C	14.54	23.98	9.82	6.23	14.39	13.79
5 ml/50°C	27.11	35.46	---	20.97	23.57	26.78
10 ml/50°C	21.03	38.34	---	15.01	21.10	23.87
15 ml/50°C	10.89	22.94	24.67	7.98	32.64	19.82

It is evident from **Table 2** that the particles are in nano size. The crystallite sizes obtained from different planes are different although they lie in nano range. The different values of crystallite sizes obtained from different crystallographic planes indicate that the powders contain different crystallite sizes. This also reflects that the XRD graph peaks are not influenced by the dispersion of the NS used as the peak positions of different planes are not shifted, and there is no specific change found in crystal structure. The XRD data have confirmed the formation of nano-HAP [19]. This reflects that the powders are not been perfectly globular but faceted. It is observed that the average crystallite size decreased with increase in NS concentration. In specific, there is an increase in average crystallite size of 15ml RcW NS with increase in temperature. So, increase in temperature leads to increase in crystallite sizes.

Scanning electron microscopic studies

The micrographs of HAP powders were examined using SEM. The SE SEM micrographs of pure HAP and 15ml RcW at 50 °C are shown in **Fig. 3.** All the powders exhibit bright contrast indicating the presence of single phase. However, it is difficult to estimate shape and sizes of the same due to agglomeration. As mentioned above, the XRD patterns also reveal the presence of single-phase HAP powders. This also points towards that the reaction is complete and no residue is left. The shapes of few isolated particles are near spherical.

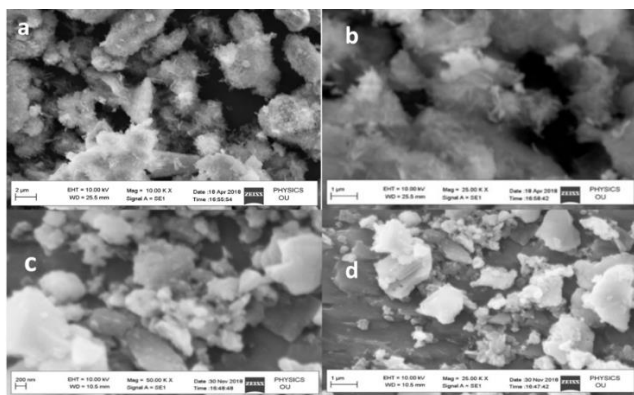


Fig. 3. SE SEM micrographs of the HAP powders: without NS (a) high and (b) low magnification and with 15 ml RcW at 50 °C (c) low and (d) high magnifications.

Small- Angle X-Ray Scattering

The sizes of HAP powders obtained in present study are measured by small angle X-ray scattering technique. The results of pure HAP, 5, 10 and 15 ml RcW at 50 °C are shown in **Fig. 4**. The nature of intensity versus scattering wave vector is same in all the cases and corresponding volume distributions reveal that the particles are poly disperse in nature (**Fig. 4**). The calculated particle sizes of poly disperse powders are given in **Table 3**. The particle sizes are different and the variation of the particle sizes lies in similar range of crystallite sizes.

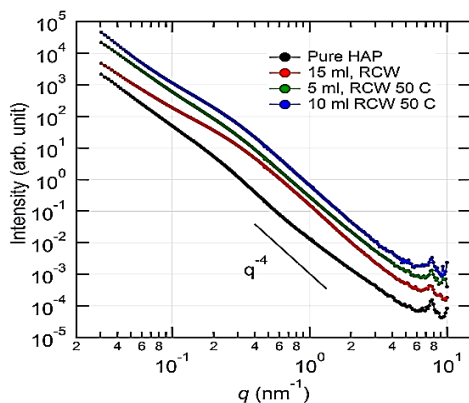


Fig. 4(a). Distributions of particle sizes (nm) of powders with pure HAP, 5ml, 10ml, 15ml RcW (NS).

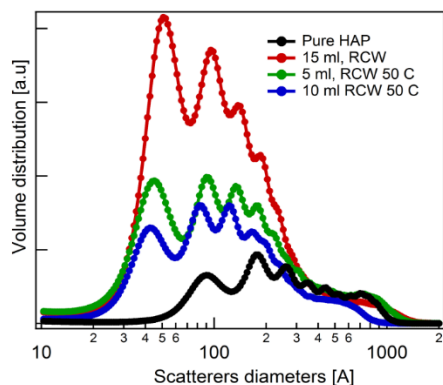


Fig. 4(b). Volume distributions of particle size with pure HAP, 5, 10, 15ml RcW (NS).

Table 3. Distributions of particle sizes (nm) of powders of pure HAP, 5ml, 10ml, 15ml RcW (NS).

Sample	S1	S2	S3	S4	S5	S6
Pure HAP	9.0	17.9	26.8	35	45	76.9
5ml, RcW	4.5	9.2	13.7	24.3	84.9	
10ml, RcW	4.3	8.5	12.2	18.2	54.8	
15ml, RcW	5.2	9.6	14.6	24.5	82	

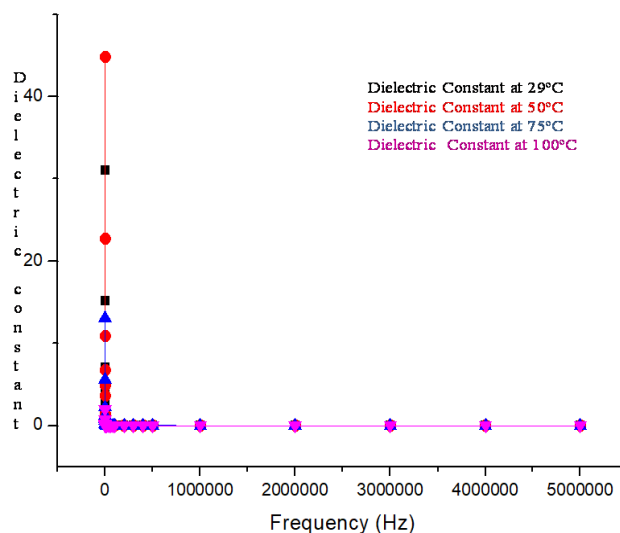


Fig. 5. Changes of Dielectric Constant when the Frequency is increasing at different temperatures.

Dielectric property

The 15 ml RcW solution at 50 °C exhibits finest crystallite and particle sizes among all the samples. This sample has therefore been used for dielectric measurement studies. The results are summed in **Table 4** and **Fig. 5**. The synthesized powder is inorganic in nature and was tested for looking up at the results of its dielectric constant. Four samples (pure HAP with NS, sample of poly acrylic acid used as binders in it, HAP sample heated till 400 °C and sample mixed with binder and heated till 400 °C) were used for the measurement of dielectric constants. All the four samples were made into pellets at five tonnes hydraulic pressure and then coated with silver paste on parallel plates at top and bottom surfaces. It is carried in a high precision impedance analyser. The pellets are tested, for getting dielectric constant keeping the frequency range, 50Hz-5MHz. The temperature variance is set at room temperature, 50, 75 and 100 °C and the derived data is taken periodically and then analysed using the following formula:

$$K = \epsilon / \epsilon_0 \quad \text{Eq. (5)}$$

where

K = Dielectric constant

$C_0 = \pi r^2/d$

$C/C_0 = \epsilon$ and

$\epsilon_0 = 8.85 \times 10^{-12} \text{F/m}$.

It is clear from the **Table 4** that the value of dielectric constant of the 15 ml RcW solution at 50 °C and 100 Hz frequency is 15.187. It has been reported that the dielectric constant of sample mixed with the binder (Poly acrylic

acid) giving ~ 15.15 at 100 Hz [20]. Therefore, the present result is in good agreement with value of dielectric constant of HAP powder reported in literature. It is also important to mention that the addition of RcW solution for the equation (3) as NS has not changed the dielectric constant value. Further, increase in frequency decreases dielectric constant significantly and it reaches close to zero (but not zero) at 5 MHz frequency. The increase in temperature also decreases the value of dielectric constants at all the employed frequency in present study.

The dielectric constant in the HAP powder prepared by 15 ml RcW NS is very low at 100 °C. This can be attributed to a relationship between frequency and dielectric constant. The rise in frequency leads to decrease in the value of dielectric constant showing that no electron transfer takes place due to poor conductivity of the material. It is also known that the conductivity of HAP material is poor and therefore the present results are not surprising [20].

Table 4. Data of Frequency and relative dielectric constant (DC) at different temperatures.

Frequency (Hz)	DC At			
	29°C	50°C	75°C	100 °C
50	31.046	44.84	13.03	1.96
100	15.187	22.75	5.56	0.77
200	7.043	10.88	2.21	0.25
300	4.422	6.76	1.25	0.11
400	3.152	4.84	0.82	0.07
500	2.429	3.65	0.59	0.04
1000	1.064	1.49	0.22	0.015
2000	0.465	0.585	0.09	0.008
3000	0.285	0.331	0.062	0.007
4000	0.199	0.225	0.049	0.0068
5000	0.152	0.164	0.043	0.0064
10000	0.064	0.064	0.031	0.0055
20000	0.028	0.028	0.025	0.0047
40000	0.013	0.014	0.019	0.0039
60000	0.008	0.0096	0.0151	0.0035
80000	0.006	0.0074	0.0132	0.0033
100000	0.005	0.0062	0.0114	0.0031
200000	0.003	0.004	0.0082	0.0028
300000	0.0027	0.0032	0.0068	0.00267
400000	0.0024	0.0029	0.0061	0.00262
500000	0.0022	0.0027	0.0055	0.00259
1000000	0.0017	0.0022	0.0039	0.00252
2000000	0.0015	0.0019	0.0028	0.00255
3000000	0.0014	0.0017	0.0022	0.00254
4000000	0.0013	0.0016	0.0019	0.00252
5000000	0.0012	0.0015	0.0016	0.00252

Fourier Transform Infrared Spectroscopy (FTIR)

The HAP powders obtained by using RcW 15ml are subjected to FTIR study. The corresponding spectrum is compared with that of known nano-HAP reference sample. The spectrum obtained in present study is similar to the spectrum of nano-HAP reported in literature [21]. It is found that both the spectra resemble each other; hence, the formation of nano-HAP is confirmed (Fig. 6). This also reflects that the powders of 15 ml RcW NS obtained in present study are nano in size. To identify the material being analysed, the synthesized 15ml RcW NS powder material is compared with spectrum obtained by known nano-HAP. Absorption bands in the range of 4000-250

wave numbers are observed. Absorption bands between 1500-4000 are due to intra-molecular phenomena and are highly specific to each material.

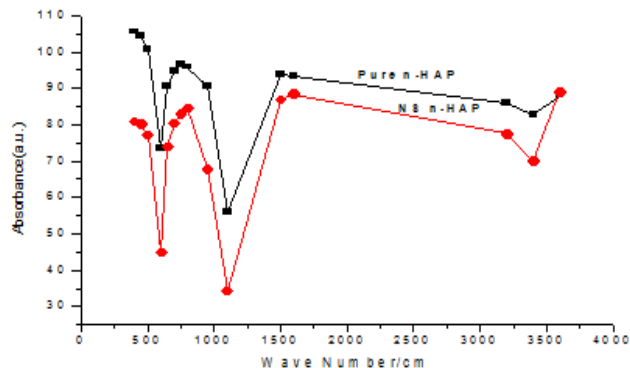


Fig. 6. FTIR Spectrum of nano-HAP and NS nano-HAP powder.

Hydroxyl stretch is observed at 3569 cm⁻¹ in the spectra of both nano-HAP and 15ml NS nano-HAP. Similar stretch is reported in synthetic commercial hydroxyapatite and natural hydroxyapatite [21]. The hydroxyl band at 3569 cm⁻¹ in the spectrum of RcW 15 ml NS apatite has higher intensity compared to that from commercial samples and also nano-HAP which is masked, may be due to RcW NS absorption. The effect of large decrease in the hydroxyl band of NS nano-HAP may be attributed to the substitution of the RcW as a NS. The small peak at 630 cm⁻¹ is characteristic of vibration of OH groups of nano-HAP confirming, the diffraction evidence [21,22]. In fact, the stretchings at 1036 cm⁻¹ and 3571 cm⁻¹ are visible for the vibrations of PO₄³⁻ and OH in lattice water, respectively [17-22]. No traces of C-H vibrations (2854 and 2924 cm⁻¹) are present, thus revealing no presence of residual NS [21,22]. It indicates the decrease of hydroxyl group because of the RcW as NS. The results obtained in present study are in agreement with data reported by Elliot et al. [21]. They have suggested the replacement of carbonate ions with hydroxyl ions.

Conclusion

Therefore, it can be concluded that, new ways of preparing eco-friendly nano sized HAP powders using natural stabilisers is going to be the most promising move in biomaterials. Consequently, this cost-effective material can of maximum utility and further can be improved with increase in Research and Development.

Acknowledgement

The Authors would like to Thank Dr. K. Suresh, Scientist E, CMCT (Centre for Material Characterisation and Testing), ARCI for the provision of SAXS facilities.

Keywords

nano – Hydroxyapatite (nano-HAP), green chemistry synthesis, Natural Stabiliser (NS), precursors.

Received: 27 May 2020

Revised: 23 October 2020

Accepted: 27 November 2020

References

1. Hench, L. L.; *J. Am. Ceram. Soc.*, **1991**, *74*, 1487.
2. Suchanek, W.; Yoshimura, M.; *J. Mater.*, **1998**, *13*, 765.
3. Peipei, Wang; Caihongli*, Haiyan, Gong; Xuerong, Jiang; Hongqiangwang; Kaixing, Li; *Powder Technology*, **2010**, 203.
4. *Journal of Material Science and Materials in Medicine*, **1997**, *8*, 1.
5. *Journal of Biomaterials Applications*, *0(0)*, 1.
6. Moshaverina, A.; Ansari, S.; Moshaverina, M.; Roohpour, N.; Darr, J.A.; Rehman, I.; *Acta Biomaterialia*, **2008**, *4*, 432.
7. Tschoppe, P.; Zandim, D.L.; Martus, P.; Kielbassa, A.M.; *J. Dent.*, **2011**, *39*, 430.
8. Erlind, Pepta, MD, Lait Kostantinos, Besharat, MD; Guido, Miglian, DDS, 2014 Jul-Sept; 5(3): 108-114 published online 2014 Nov 20 PMID: PMC425262, PMID: 25506416
9. Epple, M.; *Acta Biomaterialia*, **2018**, *77*, 1.
10. Hangoo, R.; Abbasi, F.; Rezvani, M.B.; *Scientific Research and Essays*, **2011**, *6*, 5933.
11. Growing, W.D.; Sapanis, D.C.; Deschepper, E.J.; *Journal of Esthetic and Restorative Dentistry*, **2011**.
12. Huang, S.; Gao, S.; Cheng, L.; Yu, H.; *Caries Res.*, **2011**, *45*, 469.
13. Huang, S.B.; Gao, S.S.; Yu, H.Y.; *Biomed Master*, **2009**, *3*, 03414
14. Min, J.H.; Kwon, H.K.; Kin, B.I.; *J. Dent.*, **2011**, *39*, 629.
15. Ferraz, M. P.; Monteiro, F. J.; Manuel, C. M.; *Journal of Appl. Biomat. & Biomech*, **2004**, *2*.
16. Liu, D.M.; Troczynski, T.; Treng, W.J.; *Bio Materials*, **2001**, 1721.
17. *The Royal Society*, DOI: 10.1098/rsos.180962, PMID: 30225084
18. Patterson, A. L.; *Phys. Rev.*, **1939**, *56*, 978.
19. Webster, T.J.; Siegel, R.W., Bizios, R.; *Engineering Materials*, **2001**, *192*, 321.
20. Bouyer, E.; Gitzhofer, F.; Boulos, M.I.; *J. Mater Sci Mater Med.*, **2000**, *11*, 523.
21. MichealKrumrey*; Raul Garcia-Diez; Christian Gollwitzer; Stefanie Langner, *PTB-Mitteilungen*, **2014**, *124*.
22. Suresh, S.; *Materials Physics and Mechanics*, **2012**, *14*, 145.